

Rigid Body Dynamics, Constraints, and Inverses

Hooshang Hemami
Department of Electrical and Computer
Engineering,
The Ohio State University,
Columbus, OH 43210

Bostwick F. Wyman
Department of Mathematics,
The Ohio State University,
Columbus, OH 43210

Rigid body dynamics are traditionally formulated by Lagrangian or Newton-Euler methods. A particular state space form using Euler angles and angular velocities expressed in the body coordinate system is employed here to address constrained rigid body dynamics. We study gliding and rolling, and we develop inverse systems for estimation of internal and contact forces of constraint. A primitive approximation of biped locomotion serves as a motivation for this work. A class of constraints is formulated in this state space. Rolling and gliding are common in contact sports, in interaction of humans and robots with their environment where one surface makes contact with another surface, and at skeletal joints in living systems. This formulation of constraints is important for control purposes. The estimation of applied and constraint forces and torques at the joints of natural and robotic systems is a challenge. Direct and indirect measurement methods involving a combination of kinematic data and computation are discussed. The basic methodology is developed for one single rigid body for simplicity, brevity, and precision. Computer simulations are presented to demonstrate the feasibility and effectiveness of the approaches presented. The methodology can be applied to a multilink model of bipedal systems where natural and/or artificial connectors and actuators are modeled. Estimation of the forces is accomplished by the inverse of the nonlinear plant designed by using a robust high gain feedback system. The inverse is shown to be stable, and bounds on the tracking error are developed. Lyapunov stability methods are used to establish global stability of the inverse system. [DOI: 10.1115/1.2178359]

1 Introduction

Three problems associated with rigid body dynamics are stability [1], control of constraints [2,3], and inverses for control and measurement. Stability is an issue for both the system and its inverse. The state space formulation here yields itself to systematic Lyapunov studies. The issue of noninvasive measurement of joint forces and torques [4–6] is important in the study of human location and biped models. Instruments and sensors are invasive and often undesirable. Instruments can be large, clumsy, and difficult to insert. They interfere with natural or intended function, and they may also require undesirable harnesses. A feasible alternative solution is to rely on computation and indirect measurement where quantities that are easy to measure are sensed, and measurements and computations are combined to estimate other quantities of interest [7,8].

Part of the directly and easily measurable quantities are ground reaction forces measured using instrumented force plates. Recently, better instrumentation of platforms supplies both force and moment of force measurements. Certain important parameters such as center of pressure (cop), zero moment point (zmp), and foot rotation indicator (fri) can be estimated by computation [5]. All these measurements are in the inertial (global) coordinate system (ics). Some of these quantities must be transformed to a body coordinate system (bcs), whose origin is at the center of mass, and whose axes are along the principal axes of the body [9].

The computational methods of interest here are used for calculating ground reaction forces and input torques (or moment of force).

This paper proposes the use of concepts from functional analysis [10,11] and high gain systems to construct the inverse. The

application of high gain systems to linear control systems for the purposes of compensation, robustness, stability, and design has been known for some time [12,13]. Nonlinear feedback systems with high gains can be theoretically studied within the framework of singular perturbation [14,15]. However, the emphasis and development here is on the application of inverse systems [11,12]. In this paper we use the inverse system to estimate joint forces and torques without using invasive methods.

Here it is assumed that the whole state of the system is available for input to the inverse system. The measurement of the state of the system is based on a camera-computer vision system. With some computation, we are able to arrive at the three Euler angles and their first and second derivatives with respect to time. Planar cases of a multisegment system that demonstrates these issues are studied in Refs. [7,8].

This work is relevant to diagnostic procedures where a subject stands on a platform and performs specified maneuvers or his posture is disturbed by deliberate random motions of the platform. The objective is to estimate joint or muscular forces. The three issues are platform measurements, computation methods for joint force and torque estimation, and combinations of the two. The problem requires recursive procedures and inverse system applications to multi-segment systems. For simplicity and precision, the discussions and formulations of this paper are limited to a single rigid body with one idealized (resultant) vector of torque actuation and a massless stationary foot. More realistic multi-segment models with natural attributes of muscles, ligaments, and skin tissue constitute future endeavors.

The inverse construction has other applications in understanding control mechanisms used by natural systems.

Maintaining upright stability and generating purposeful movements require knowledge of the movement of various body segments. The sensory modalities, namely, the proprioceptive, visual, and vestibular mechanisms, provide the angles and angular velocities [16,17]. Some of the angles and angular velocities are sensed directly (e.g., head velocity by the vestibular system) while others are sensed indirectly (e.g., ankle angle by the proprioceptive and somatosensory receptors). Based on this information, the central

Contributed by the Applied Mechanics Division of ASME for publication in the JOURNAL OF APPLIED MECHANICS. Manuscript received December 3, 2004; final manuscript received December 19, 2005. Review conducted by I. Mezic. Discussion on the paper should be addressed to the Editor, Prof. Robert M. McMeeking, Journal of Applied Mechanics, Department of Mechanical and Environmental Engineering, University of California – Santa Barbara, Santa Barbara, CA 93106-5070, and will be accepted until four months after final publication of the paper itself in the ASME JOURNAL OF APPLIED MECHANICS.

nervous system decides which muscles must be activated to generate the desired joint motions. Although the exact timing and magnitude of muscle activation are most likely determined locally, a more global control strategy is necessary to coordinate movements of different body segments. Determination of joint torques is the essential first step to understand the feedback mechanisms that map the sensory information onto the motor outputs.

A related application of inverse system methodology is to the concept of preprogramming in the central nervous system (CNS). Horak and Nashner [18] have proposed a hierarchical organization of postural control mechanisms in which a limited set of preprogrammed motor routines is used to generate multidimensional movements. In the most basic form, these movements take the form of ballistic movements where the limb trajectories are determined by the initial burst of the neural activity [19]. The ballistic movements are required for executing fast movements. Postural adjustments seem to fall under the category of “planned” movements. For these movements, the motor control system operates in a closed-loop manner to achieve a greater accuracy while minimizing the effects of neural delays. This view of the postural control system requires the CNS to maintain an approximate model of the intended movement and the internal system dynamics [20]. This model is developed through a “learning” process. During the execution of planned movements, the “stored” or “learned” movements are constantly compared with the information arriving from the sensory mechanisms. As long as the intended and actual movements are within a tolerance limit, the programmed routines can proceed without intervention. When conflicts arise, such as when an unanticipated postural disturbance is encountered, the CNS will first attempt to modify the parameters of the preprogrammed routine to achieve the intended movement. If the conflict persists, such as when a lesion develops in the sensorimotor mechanisms, the CNS must actively use the available sensory feedback mechanisms to maintain stability while at the same time modifying its internal model of the system dynamics. The cost of such conflicts is increased response time and reduced accuracy of resulting movements. We hope to apply our methods to the preprogramming situation in a later paper.

2 Rigid Body Dynamics

Rigid body dynamics and control can be formulated with the recently developed and elegant geometric tools [21,22]. Here we apply the Newton-Euler method in order to derive the equations of a single free rigid body. Let Θ and Ω be, respectively, the Euler angles and the angular velocity vector of the body expressed in the previously defined body coordinate system (bcs). Let X and V be the translational vectors of position and velocity of the center of gravity of the body, expressed in the inertial coordinate system (ics) system. With reference to vector R , we define the skew symmetric 3×3 matrix \check{R} [23,24]. The vectors of force G and Λ are, respectively, the gravity vector and an equivalent or resultant vector of all forces [9] acting on the rigid body. Similarly N is an equivalent or resultant couple of all forces acting on the rigid body. Alternatively speaking, N is the sum of all the couples: stabilizing couples, trajectory control couples, and the moment of all forces acting on the rigid body. The asymptotic stability of the rotational system by nonlinear feedback has been discussed in Refs. [1,23], and will be briefly presented later in this paper. The coordinate systems are defined in the Appendix . Based on these simplifications, the equations of motion of the single rigid body are [25,26]

$$\begin{aligned} \dot{\Theta} &= B(\Theta)\Omega \\ J\dot{\Omega} &= f(\Omega) + N \\ \dot{X} &= V \end{aligned} \quad (1)$$

$$m\dot{V} = G + \Lambda$$

where J is the diagonal moment of inertia matrix, expressed in bcs, B is a 3×3 matrix defined in the appendix , and where

$$f(\Omega) = \check{\Omega}J\Omega$$

2.1 Rolling and Gliding. When a rigid body contacts another rigid body, the two surfaces can be approximated by rigid body spheres. As an example, suppose a player kicks a soccer ball such that the front of the shoe touches the ball, i.e., a toe kick takes place. The collision can be approximated by the viscoelastic collision of one sphere with another. When the player kicks the ball with the top of his foot, the foot surface can be approximated by a plane, a cylinder, or a sphere.

Let a uniformly dense rigid body sphere with radius Q be centered at the origin of the inertial system. This means the center of the sphere and its center of gravity coincide. Let another uniformly dense sphere of radius q roll or glide on the first sphere. The contact eliminates one of the three degrees of translational freedom of the moving sphere. At the point of contact, the two spheres' surfaces can be approximated by their respective tangent planes. This means two of the degrees of freedom of the moving rigid body are thus constrained. The remaining degree of freedom is the self-rotation of the rigid body along the center to center line of the two spheres. In order to control the motions of gliding and rolling, the equations of constraint are needed [2,3].

Let Eq. (1) describe the motion of the moving sphere. In both gliding and rolling, the two spheres' being in contact is described by the holonomic constraint

$$X'X - (Q + q)^2 = 0 \quad (2)$$

Alternatively, this equation is written as

$$X'\dot{X} = 0 \quad (3)$$

2.2 Pure Gliding. In gliding a fixed vector S in the body coordinate system (bcs) keeps contact with the stationary sphere. Let p and \dot{p} be, respectively, the vector of the contact point, and its velocity in ics:

$$p = X + A(\Theta)S \quad (4)$$

$$\dot{p} = \dot{X} + A(\Theta)\check{\Omega}S$$

In gliding, the velocity of the moving body at the point of contact is in the tangent plane of the stationary sphere, therefore the inner product of \dot{p} and X is zero. Also the velocities of the point of contact and the center of gravity of the moving sphere are in parallel, because the instantaneous center of rotation of the moving sphere is the origin of the ics, namely, the center of the stationary sphere. The latter requirement means

$$\dot{p} = [q/(Q + q)]\dot{X} \quad (5)$$

From Eqs. (4) and (5), the constraints for gliding can be obtained

$$q\dot{X} + (Q + q)A(\Theta)\check{\Omega}S = 0 \quad (6)$$

2.3 Rolling Motion. Rolling is a special case of the more general class of nonholonomic systems [2], Chap. 3. Nonholonomic constraints either appear as part of the structure of a mechanical system, or are part of the specifications for control in order to simplify implementation of coordinated movement.

In rolling motion of the sphere, the instantaneous center of rotation of the moving sphere is the point of contact. From this information, and the above equations, one can obtain the three constraints for rolling

$$Q\dot{X} + qA(\Theta)\dot{\Omega}A'(\Theta)X = 0 \quad (7)$$

With the equations of the rigid body and the constraints given above, the questions of the derivation of the necessary forces of constraint in order to maintain the constraint, and deriving feedback in order to implement the constrained motion can be carried out as described in Refs. [2,3]. These issues are not further pursued here.

2.4 Illustrative Example. Suppose the motion is limited to the x_1x_3 plane. Suppose further that the spheres are initially stacked on the top of each other so that

$$p(0) = [0, 0, Q]'$$

and

$$X(0) = [0, 0, Q + q]'$$

The equations of motion can be derived by setting

$$x_2 = \omega_1 = \omega_3 = 0$$

The gliding constraints in this case become

$$\dot{x}_1 = (Q + q)\dot{\theta}_2 \cos(\theta_2) \quad (8)$$

$$\dot{x}_3 = -(Q + q)\dot{\theta}_2 \sin(\theta_2)$$

The rolling constraints in this case become

$$Q\dot{x}_1 = q\dot{\theta}_2 x_3 \quad (9)$$

$$Q\dot{x}_3 = -q\dot{\theta}_2 x_1$$

2.5 Rotational Motion. Consider the rigid body formulation in Eq. (1). Suppose the center of gravity is fixed in the ics, and only the rotational motion is of interest. For an alternative state space formulation of rigid body dynamics, see [24].

It is assumed here that the range of Θ is limited such that the Lipschitz condition is satisfied. With the latter assumption, it has been shown that with state feedback

$$N = -B'(\Theta)K_1\Theta - L_1\Omega$$

where both K_1 and L_1 are positive definite [23] that the rotational rigid body motion is asymptotically stable. Isidori ([24], Lemma 2, Appendix B, Sec. 2.2), and Khalil ([15], Chaps. 5,6) have shown that the system is stable under nonvanishing persistent disturbance. Equivalently, one can prove that the rotational system of Eq. (1) produces uniformly bounded outputs when the inputs is uniformly bounded. This means the above system is bounded-input bounded-output (BIBO) stable.

3 Inverse System

3.1 Basics. The inverse system can be formally designed based on concepts from functional analysis [11] and nonlinear operator algebra [10] or from more recent geometrically and algebraically based methods [24,27]. The functional analysis method for computation of the inverse is based on feedback [11,12]. Since natural, robotic, and humanoid systems use feedback for stability, control, and tracking, use of methods based on feedback appear to be more natural, intuitive, and less sensitive to system parameter variations. Besides, the natural structure of the system to be inverted is used for arriving at the inverse. In addition, it is important that the inverse system be stable. It is not clear, from the development of the modern techniques [24,27], whether additional stabilizing mechanisms are needed for the inverse system, and how these additional mechanisms may disturb the inverse system, and interfere with its operation. The approach here also does not require development of zero dynamics [24] since it is assumed that the state and hence the initial state are

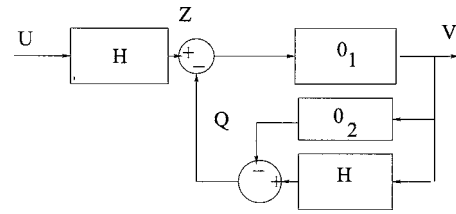


Fig. 1 A continuous nonlinear system H , and its inverse composed of a replica of H and two operators O_1 and O_2

known for the inverse system.

The method developed below considers global stability and inversion issues simultaneously. It is shown how global stability may effect the performance of the inverse system, and how an exact inverse may affect global stability. First a brief introduction is made to the feedback structure of the general inverse systems. The structure is applied to the rotational dynamics of a single rigid body next. Global stability is guaranteed by perturbation of the inverse.

Let U be the input and Z the state output of a nonlinear continuous invertible system described operationally by a nonlinear operator H . Following the formulation of [10,11], the system can be described by the following equation:

$$Z = HU \quad (10)$$

We assume that conditions for the existence and uniqueness of the solution for Z , and the inverse system [11] are satisfied. Let O_1 and O_2 be two operators such that the product of the two operators is equal to identity

$$O_1O_2 = I$$

where I is the identity operator. The block diagram of the system above followed by the inverse system is given in Fig. 1. The output of the inverse system is V . The equations of the inverse system are

$$Q = (H - O_2)V \quad (11)$$

$$V = O_1(Z - Q)$$

Elimination of Q from the above two equations results in

$$Z = HV \quad (12)$$

From Eqs. (10) and (12), it follows that

$$U = V$$

In other words the tandem connection of the system and its inverse results in the identity operator. In practical terms if Z is the measured state of a musculo-skeletal system, and if it is desired to estimate the input muscular vector of forces, i.e., vector U , the output V of the inverse system is an estimate of the unknown muscular forces. This inverse system can be constructed by the block diagram of Fig. 1, and requires an exact replica of the original system, i.e., the operator H .

3.2 Construction. We construct here the inverse of the rotational system discussed above. The inverse system is based on the above nonlinear operator principles and is defined by a nonlinear feedback system with one forward component and two feedback components as shown in Fig. 1.

Consider the rotational system alone

$$\dot{\Theta} = B(\Theta)\Omega \quad (13)$$

$$J\dot{\Omega} = f(\Omega) + U$$

Consider the operator H to be represented by Eq. (13). The state

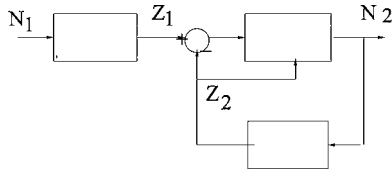


Fig. 2 The free rigid body in rotation with input N_1 and output Z_1 , (Eq. (13)) in series with the nonlinear inverse with high gain feed forward and a model of the system in the feedback path

$$Z = [\Theta', \Omega']'$$

and the input is

$$U$$

In this formulation Z is of dimension six, and U of dimension three. For ease of formulation, we assume U is a sum of two couples so that it is also of dimension six

$$U = [V_1', V_2']'$$

The feed forward component of the inverse system is a nonlinear amplifier with high gain. Let K and L be two 3×3 positive definite matrices, and define the 6×6 positive definite matrix G_1 with K and L along its diagonal

$$G_1 = [K, 0, 0, G] \quad (14)$$

Similarly, with B as defined in Eq. (1), and I as the 3×3 identity matrix, define the 6×6 matrix α as follows:

$$\alpha = [B', 0, 0, I] \quad (15)$$

With these definitions, the operator O_1 is defined

$$O_1 = \alpha G_1 \quad (16)$$

The operator O_2 is simply the inverse of O_1

$$O_2 = (G_1)^{-1} (\alpha^{-1}) \quad (17)$$

The other feedback component is a replica of the original system slightly modified to account for adding together the vectors N_1 and N_2 as a single input vector.

$$\dot{\Theta}_2 = B(\Theta_2) \Omega_2 \quad (18)$$

$$J\dot{\Omega}_2 = f(\Omega_2) + V_1 + V_2$$

3.3 Stability. Stability of the inverse system is proven here. From the derivation of the inverse, it follows that the inverse system above is BIBO stable [15].

It is relatively easy to consider asymptotic stability of the inverse system as a high gain system by setting

$$O_2 = 0.$$

We show here that this approximate inverse system is asymptotically stable. The block diagram of the rotational system and its inverse is shown in Fig. 2. Let the Lyapunov function for the inverse system be the sum of the kinetic and elastic energy of the system

$$v = 0.5 \Omega_2' J \Omega_2 + 0.5 (\Theta_2)' K (\Theta_2). \quad (19)$$

It is easy to show that the derivative of the Lyapunov function is

$$\dot{v} = -\Omega_2' L \Omega_2 \quad (20)$$

This derivative is negative semidefinite, but a nonzero Θ cannot be a solution to the inverse system equation. Therefore by invoking La Salle's Theorem [28], the global stability of the inverse system is assured, subject to the limited range of Θ due to the Lipschitz condition.

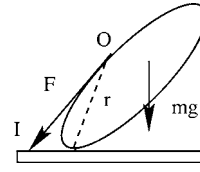


Fig. 3 The inverted pendulum in contact with a massless foot. An actuator with origin O on the pendulum and insertion point on the foot applies a force F to the pendulum along the line OI .

3.4 Approximate Inverses. Due to the large choices for O_1 and O_2 , one can develop a range of inverses. Of particular interest are those when a fraction of O_2 is used in the feedback path, namely, an amplifier with a small gain precedes or follows the operator O_2 .

Assume a particular O_1 is chosen (see examples later). Let ϵ be a number

$$0 \leq \epsilon \leq 1$$

and let

$$E = \epsilon O_2$$

It can be shown that the system that is inverted is $H - (1 - \epsilon) O_2$. This means, for a given H and given ϵ the operator O_1 can be selected sufficiently large enough and, consequently, the operator O_2 sufficiently small enough for the error in V to be acceptable. The computational detail of how to carry this step out are not presented here.

Another bound can be established for the steady state system state error. Assuming that the gains K and L are sufficiently high so that $U = V$, and letting E_1 and E_2 be, respectively, the errors in angle Θ and angular frequency Ω , it follows that

$$V_1 + V_2 = B' K E_1 + L E_2 \quad (21)$$

From this equation, approximate upper bounds can be established for the errors

$$|E_1| = < K^{-1} |V_1 + V_2|,$$

and

$$|E_2| = < L^{-1} |V_1 + V_2|$$

This means that the higher the gains K and L are, the smaller the error. Of course, higher values for the gains demand higher sampling rate, and therefore more on-line computations.

4 The Inverted Pendulum

Next, a rigid body is considered [23] as shown in Fig. 3. It is assumed that a point on the body with coordinates

$$R = [0, 0, -r]$$

in the body coordinate system is attached to the origin of the ics, and that the vector of constraint force at the point of attachment, expressed in the ics is Λ . A system of muscle-like actuators connect the rigid body to a weightless foot. One actuator is shown in Fig. 3. Let the resultant moment of all the actuator forces, relative to the contact point, as shall be described later, be vector N in the bcs. Let the sum of the actuator forces, in the ics be H . The rotational motion of the rigid body about its center of gravity is governed by

$$\dot{\Theta} = B(\Theta) \Omega \quad (22)$$

$$J\dot{\Omega} = f(\Omega) + N + \check{R} A' \Lambda$$

The translational motion of the center of gravity is governed by

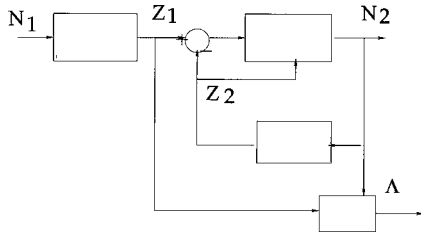


Fig. 4 The inverted pendulum with input N_1 and output Z_1 (Eq. (22)) in series with the nonlinear inverse with high gain feed forward path and a model of the system in the feedback path. The estimate of total input torque is the output N_2 . The ground reaction force Λ (Eq. (23)) is constructed from Z_1 and N_1 .

$$m\dot{V} = G + H + \Lambda$$

where G is the gravity vector in ics. It can also be shown [1] that the latter equation can be rewritten, involving variables Λ and $\dot{\Omega}$

$$\Lambda + G + H = -mA(\check{R}\check{\Omega})\Omega + mA\check{R}\dot{\Omega} \quad (23)$$

Equations (22) and (23) can be simultaneously solved for $\dot{\Omega}$ and Λ . The solution for $\dot{\Omega}$ is the state space equation for the pendulum relative to a body coordinate system whose origin is at the base, and whose axes are parallel with the principal axes.

$$\dot{\Theta} = B(\Theta)\Omega \quad (24)$$

$$J_b\dot{\Omega} = [f_b(\Omega) + N - \check{R}A'G]$$

Here J_b is the moment of inertia matrix relative to a (principal axes) body coordinate system centered at the point of attachment or contact; and

$$f_b = \check{\Omega}J_b\Omega$$

The solution for Λ is the force of constraint as a function of inputs, i.e., N and gravity, and the state (i.e., Θ and Ω). For ease of reference the latter two equations are symbolically written as

$$\dot{\Omega} = O_3(\Theta, \Omega, N_t) \quad (25)$$

$$\Lambda = O_4(\Theta, \Omega, N_t)$$

where N_t is the total applied torque to the pendulum, including stabilizing torques, actuating torques, gravity, etc.

4.1 The Inverse System. The problem of the inverse system, defined before, is slightly generalized here: Given the quantities Θ , and Ω , estimate N_t and Λ . We assume again that $H=0$. This means that the resultant torque of these forces, namely, N is the same whether it is relative to the center of gravity of the inverted pendulum or the point of contact.

Suppose the same inverse system as in Fig. 2 is utilized, it follows that

$$N_t = N_2 \quad (26)$$

$$\Lambda = O_4(\Theta, \Omega, N_t)$$

It is clear from Eq. (23) that Λ can be computed from the state Z_1 , and the derivative of Ω with respect to time. This alternative way to arrive at an expression for Λ is to compute it from Eq. (1)

$$\Lambda = m\dot{V} = -G + m[A\check{R}\dot{\Omega} - A\check{\Omega}^2R] \quad (27)$$

The structure of the inverse system is shown in Fig. 4.

4.2 Measurement of N and Λ . It is instructive to consider direct measurement of the torque N and force Λ . For this purpose, an instrumented platform is needed on which the inverted pendu-

lum is installed. The instruments measure the total torque and force applied by the rigid body to the platform. Here, we consider the stationary case. For a discussion of the dynamic case, see [5]. For a detailed exposition of the planar case of the inverse system in a multilink biped in the sagittal plane see [7,8]. This means the platform instrumentation avails N_1 and Λ . Let us assume that the pendulum is attached to the ground by a massless and stationary foot. Further, if the foot is not attached rigidly to the ground, we assume that the friction forces are large enough, (i.e., larger than the constraint forces) so that the foot does not move or slide. Suppose there are six actuators connecting the inverted pendulum to the foot—each agonist-antagonist pair providing control for the roll, pitch and yaw movements. The arm of the actuator force, shown in Fig. 3 is vector r , expressed in the bcs that extends from the contact point to the origin of the actuator, i.e., point O . Suppose the force of this actuator, namely, vector F , is expressed in the ics. The torque of this actuator, relative to the point of contact, expressed in bcs, is

$$\check{R}A'F$$

The vector N is the sum of the six torques. One needs the points of origin and insertion of the six actuators in ics, in order to arrive at the direction of these forces, and one needs the insertion coordinates and the contact point coordinates, in the bcs, in order to arrive at the R vectors. The massless foot, in turn is acted upon by $-N$, expressed for convenience, in the ics. Suppose, the interaction between this foot and the ground is by a set of n discrete three-vector ground reaction forces: τ_i where index i runs from 0 to n . These forces act on the bottom of the foot, respectively, at vectors s_i in the ics. Let the ankle joint apply a single force of constraint Λ to the massless foot. The equilibrium of the foot results in the sum of the ground reaction forces being equal to Λ plus the sum of the actuator forces; and the moment of all the ground reaction forces relative to the point of contact, i.e., the origin of the ics, being equal to N , expressed in the ics. When the sum of the actuator forces is equal to zero: $H=0$, the sum of the ground reaction forces under the foot is exactly equal to Λ .

Now, from the instrumentation on the platform, the sum of the ground reaction forces under the foot and the moment of all these reaction forces relative to the point of contact can be computed. This means the quantities Λ and N can be measured from the instrumentation on the platform.

The main point of the discussion here is that the inverse of the inverted pendulum is derived with the dynamics of the inverted pendulum formulated about the point of contact. The inverse system estimates the total torque applied to the rigid body. To arrive at the applied torque, the contribution of the torque of the constraint force Λ must be subtracted.

5 Simulation Results

Several computer simulations are presented here in order to demonstrate the efficiency, viability, and feasibility of this formulation. The first simulation deals with a body rotating about its center of gravity. The numerical parameters and gains are listed in the Appendix .

5.1 Rotating Rigid Body. The rotational rigid body motion about its center of gravity is considered. First, state feedback of the position Euler angles and angular velocity vector, i.e., Ω is used from Sec. 2.5 to stabilize the motion. The stabilizing position and velocity gains are the 3by3 diagonal matrices: $K_1 = \text{Diag}(400, 400, 320)$, and $L_1 = \text{Diag}(60, 60, 42)$.

Three impulsive torques are assumed to have been applied to this rigid body in order to set up the following initial conditions:

$$[0, 0, 0, 2.5, -2.5, 2.5]$$

With these initial states the behavior of the system is simulated for about 0.1 s. The vector of total torque acting on the body and the state are computed and also recorded. This transient behavior of

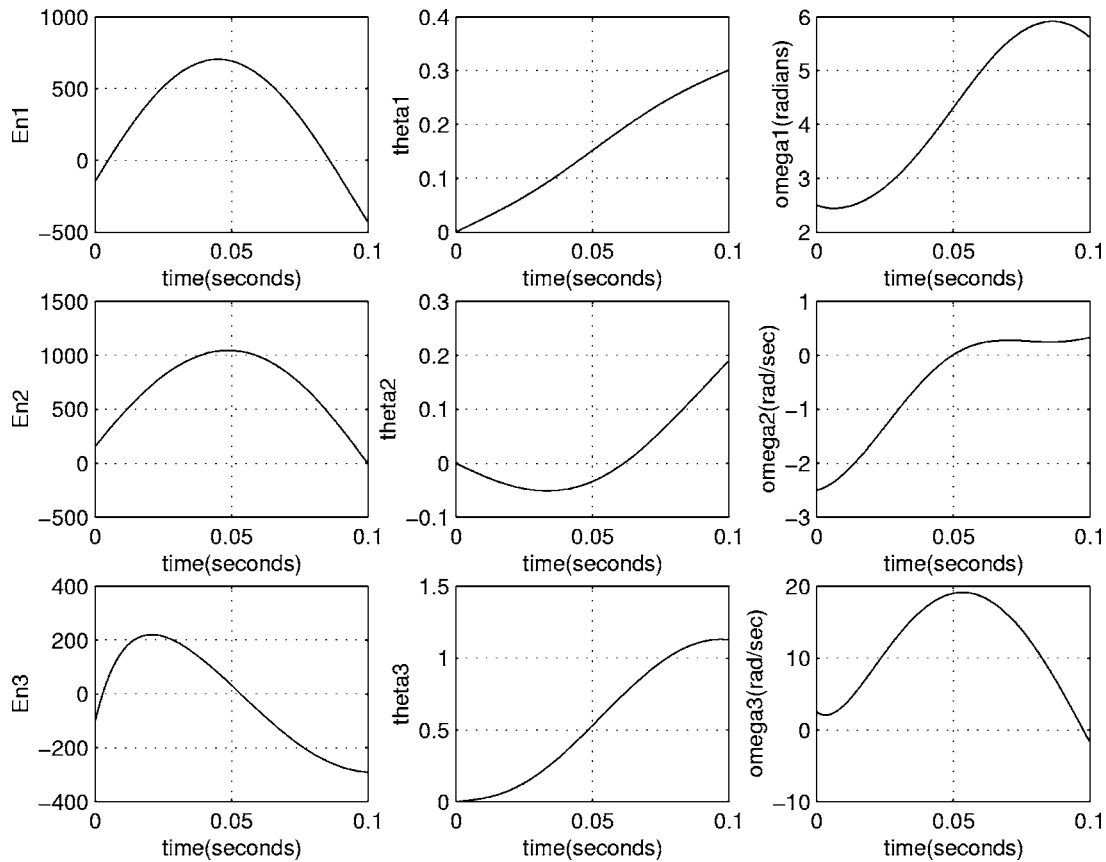


Fig. 5 The input torque E_n , the angles, and angular velocities as functions of time for one rigid body anchored at its center of gravity

the stabilized rigid body is documented in Fig. 4. The figure shows the input torques, the angles Θ , and angular velocities Ω , all as functions of time. The angles and angular velocities are now input to the inverse system. It is assumed that the physical parameters of the inverse system are the same as those of the rotating rigid body. The gains in the forward loop, namely, K and G in Eq. (14) are chosen to be the same diagonal 3×3 matrix, i.e.,

$$K = \text{Diag}(10000, 5000, 500)$$

and

$$G = \text{Diag}(10000, 5000, 500)$$

The output of the inverse system is given in Fig. 5, along with the error signals in Θ and Ω . The comparison of the actual and the estimated torques in the previous two figures show that the inverse system is very good in tracking the torques. There are initial errors in all three torques because, for the inverse system, the initial states and outputs are all zero. However, as can be seen in the figure, the tracking of the torques is very good after about 0.004–0.008 s.

5.2 The Inverted Pendulum. In this simulation, the rigid body is anchored to the ground at a point with coordinates R as an inverted pendulum. The initial conditions are all zero. It is subjected to stabilizing feedback torques as before. These feedback gains are given by the diagonal 3×3 matrices: $K_2 = \text{Diag}(1200, 1200, 960)$, and $L_2 = \text{Diag}(180, 180, 126)$.

In addition, there are periodic torques acting at the base of the pendulum for one second. The three components of the torque vector are equal

$$n = 1000 \sin(10\pi t).$$

The input torques and the ground reaction force are to be the desired quantities to be estimated. They are recorded and plotted in Fig. 6. The angles and angular velocities of the inverted pendulum are the outputs of the system and are plotted in Fig. 7. It can be seen that the system assumes a steady state in less than 0.2 s. The structure of the inverse is taken as that of Fig. 8. The gains in the forward loop, namely, K and G in Eq. (14) are chosen to be the same diagonal 3×3 matrix, i.e.,

$$K = \text{Diag}(17232, 15232, 200)$$

and

$$G = \text{Diag}(17232, 15232, 200)$$

The inputs to this inverse system are the position angles and the angular velocities recorded as outputs of the previous simulation. With these inputs and zero initial conditions, the inverse system is simulated for one second. The outputs of the inverse system are the ground reaction forces and the total torques acting on the system. These estimated total torques and estimated ground reaction force are shown in Fig. 9. The state trajectories of the inverse system are shown in Fig. 10.

6 Conclusions

We have considered dynamics, inverse, and control of a single rigid body system with constraints. We have developed a methodology to construct Lyapunov stable inverses for these systems. The procedures here can be extended to multi-body systems that are better approximations to systems involved in medicine, robotics and human movement.

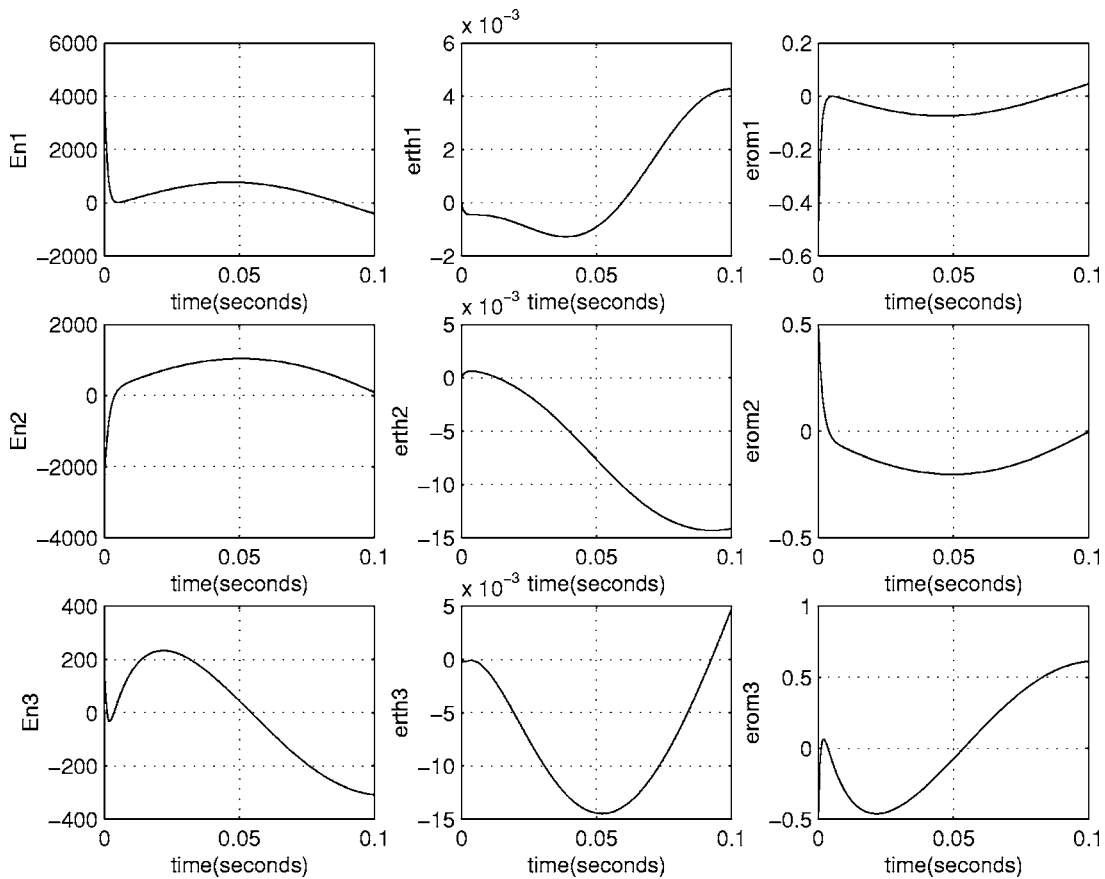


Fig. 6 The estimated torques as outputs of the inverse system as functions of time. The error signals in Θ and Ω , as inputs to the high gain forward component of the inverse are also plotted as functions of time.

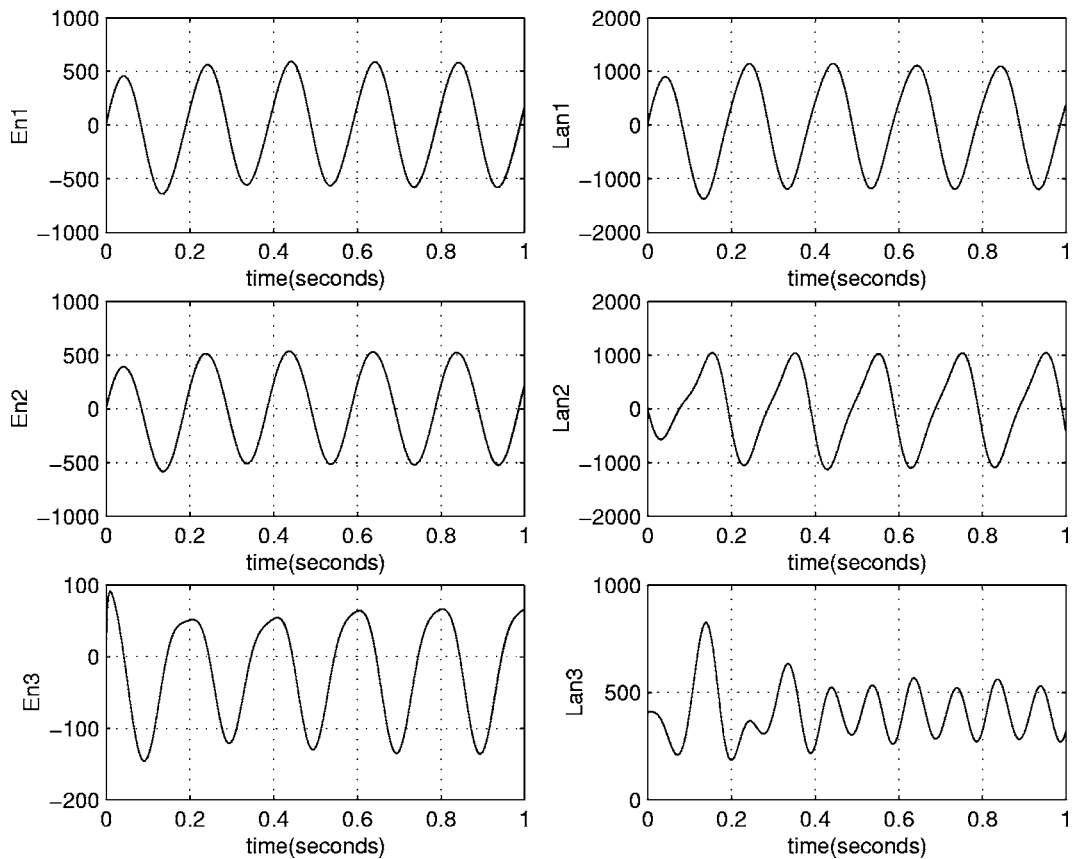


Fig. 7 The total applied torques to the inverted pendulum, and the resulting ground reaction force as functions of time

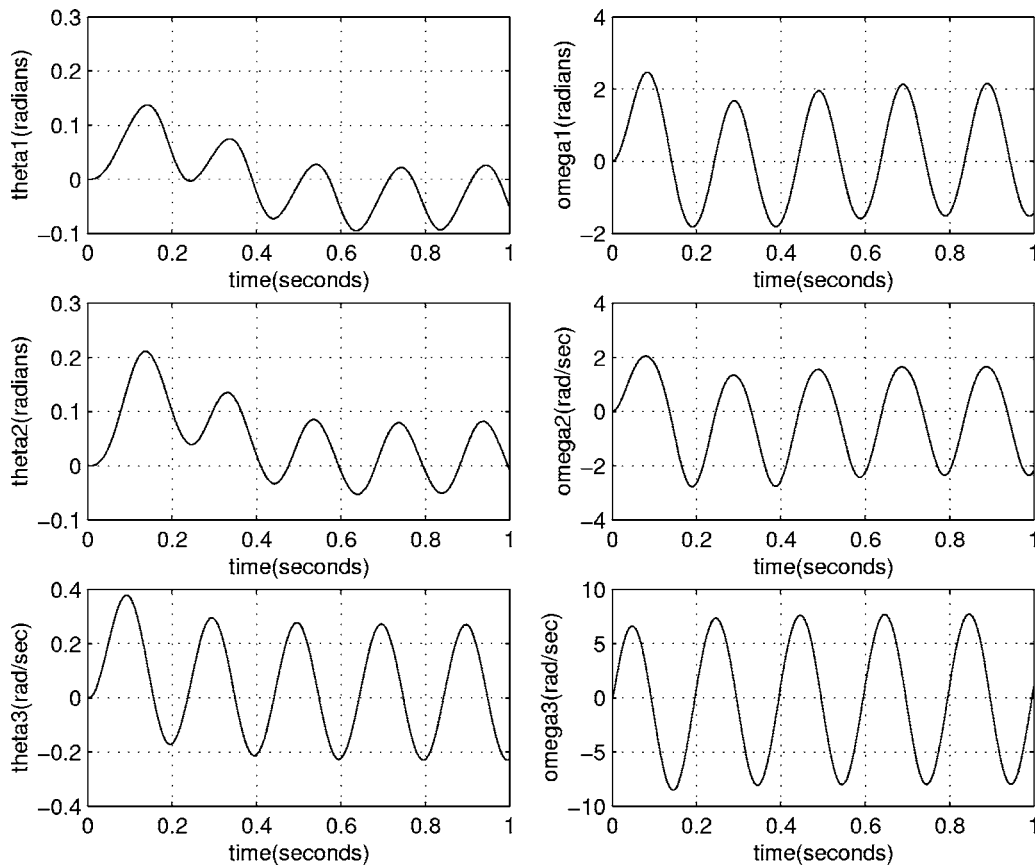


Fig. 8 The state trajectories of the inverted pendulum: Θ and Ω as functions of time

The computational methods pose interesting challenges for multilink three-dimensional systems:

1. If the trajectories of the state of the system (i.e., position and velocity variables) and either the input torques or the accelerations are known, the ground reaction and joint forces should be computable as shown in Ref. [2] for very simple cases.
2. The computation of input torques to the multilink system, in order for the system to follow a desired trajectory, or the estimation of such torques, when the trajectories are known, can be implemented with inverses.
3. In certain instances, both the trajectories and the constraint forces (ground reaction forces are an example) are specified. This class of problems has not been studied from a theoretical point of view. Some heuristic methods have been applied before [29]. The problem is tractable if there are a sufficient number of inputs to control the forces and the trajectories.

We have shown relevance of functional analysis, inverse system theory, and high gain systems to formulating and solving the above problems.

Acknowledgment

The authors would like to thank the reviewers for their careful reading of the manuscript, and for their valuable and constructive criticism.

Appendix

1 Single Rigid Body

The inertial coordinate system is defined as follows. The x_1 axis is to the front of a biped, or the front of an airplane—the longi-

tudinal axis. The x_2 coordinate is in the direction of the extended left hand of the biped or the pitch axis of the airplane. The third axis x_3 is vertically upward, the yaw axis in an airplane. The Euler angle sequence corresponds to roll, pitch, and yaw.

Let A be the 3×3 orthonormal matrix that transforms vectors from the bcs to ics. The inverse of A is A' . The matrices $A(\Theta)$, $B(\Theta)$, and $\tilde{\mathcal{R}}$ are given below.

Let $A_1(\theta_1)$, $A_2(\theta_2)$, and $A_3(\theta_3)$ be defined by

$$A_1(\theta_1) = \begin{bmatrix} 1 & 0 & 0 \\ 0 & \cos \theta_1 & -\sin \theta_1 \\ 0 & \sin \theta_1 & \cos \theta_1 \end{bmatrix}$$

$$A_2(\theta_2) = \begin{bmatrix} \cos \theta_2 & 0 & \sin \theta_2 \\ 0 & 1 & 0 \\ -\sin \theta_2 & 0 & \cos \theta_2 \end{bmatrix}$$

$$A_3(\theta_3) = \begin{bmatrix} \cos \theta_3 & -\sin \theta_3 & 0 \\ \sin \theta_3 & \cos \theta_3 & 0 \\ 0 & 0 & 1 \end{bmatrix}$$

Now $A(\Theta)$ can be defined

$$A(\Theta) = A_1(\theta_1)A_2(\theta_2)A_3(\theta_3)$$

The matrix $B(\Theta)$ is given by

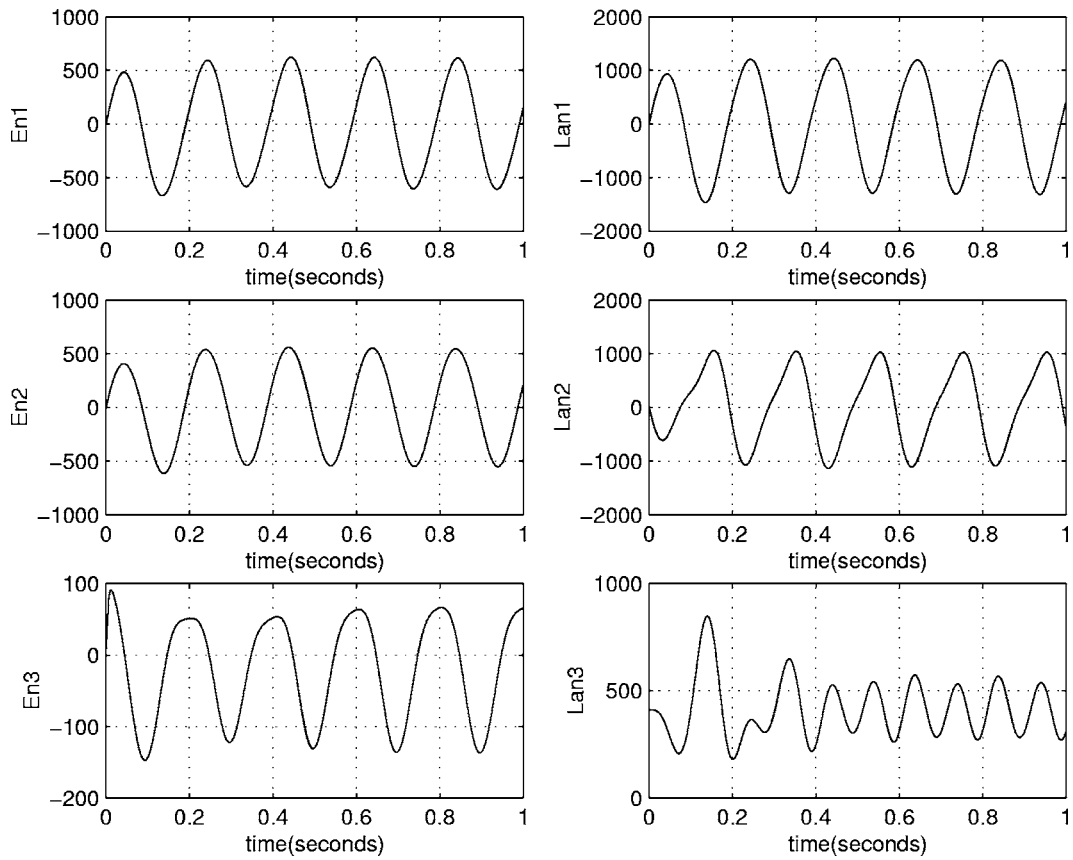


Fig. 9 The estimated total torque applied to the inverted pendulum, the estimated ground reaction forces as functions of time

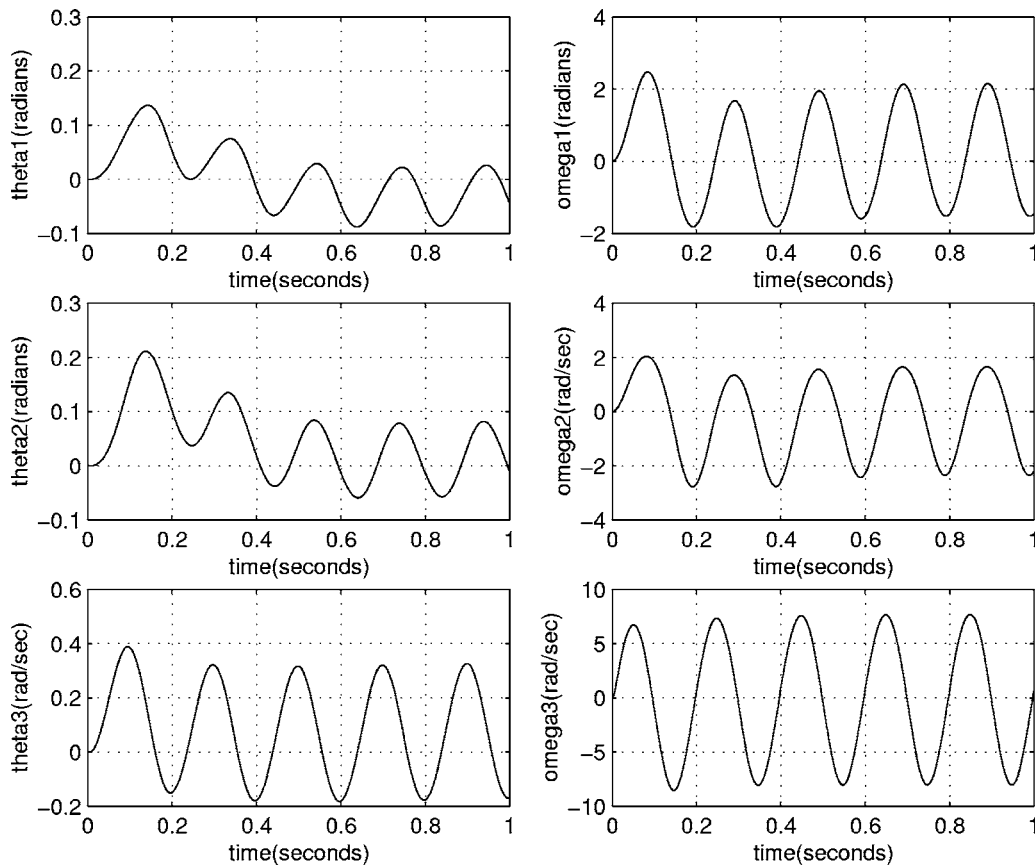


Fig. 10 The state of the estimator as a function of time

Table 1 Definition, symbols, and numerical values for one rigid body

	Symbol	Value	Unit
Mass.	m	41.00	Kg
Principal moment of inertia	j1	10.0	Kg m ²
Principal moment of inertia	j2	8.0	Kg m ²
Principal moment of inertia.	j3	0.4	Kg m ²
Center of gravity	l	0.42	m
Gravity constant	g	10.0	m/s ²

$$B(\Theta) = \begin{bmatrix} \cos \theta_3 & -\sin \theta_3 & 0 \\ \cos \theta_2 & \cos \theta_2 & 0 \\ \sin \theta_3 & \cos \theta_3 & 0 \\ -\sin \theta_2 \cos \theta_3 & \sin \theta_2 \sin \theta_3 & 1 \\ \cos \theta_2 & \cos \theta_2 & 1 \end{bmatrix}$$

It is to be observed that matrix B is of finite norm only for a limited range of θ_2 , i.e., θ_2 must lie in the open interval: $-\pi/2$ and $+\pi/2$. This is the range for which the Lipschitz condition holds. For θ_1 and θ_3 , respectively, corresponding to roll and yaw, the range is from $-\pi$ to $+\pi$ - corresponding to the range for the physical three-dimensional world. All the development and results in this paper are limited to these ranges.

Let vector R have components r_1, r_2 , and r_3 . The skew symmetric matrix \tilde{R} is defined as

$$\tilde{R} = \begin{bmatrix} 0 & -r_3 & r_2 \\ r_3 & 0 & -r_1 \\ -r_2 & r_1 & 0 \end{bmatrix}$$

2 Numerical Values

The definitions, symbols, and numerical values for a single rigid body system [23,30] are given in Table 1.

References

[1] Hemami, H., and Utkin, I., 2002, "On the Dynamics and Iyapunov Stability of Constrained and Embedded Rigid Bodies," (unpublished).
 [2] Hemami, H., and Wyman, B., 1979, "Modeling and Control of Constrained Dynamic Systems With Application to Biped Locomotion in the Frontal Plane," IEEE Trans. Autom. Control, **24**, pp. 526–535.
 [3] Hemami, H., and Wyman, B., 1980, "Indirect Control of the Forces of Constraint in Dynamic Systems," J. Dyn. Syst., Meas., Control, **24**(4), pp. 355–360.
 [4] Winter, D., 1990, *Biomechanics and Motor Control of Human Movement*, Wiley, New York.

[5] Goswami, A., 1999, "Foot Rotation Indicator(fri) Point: A New Gait Planning Tool to Evaluate Postural Stability of Biped Robots," Proc. ICRA 1999, Detroit, Vol. 1, IEEE Robotic Society, New York, pp. 47–52.
 [6] Dariush, B., Hemami, H., and Parnianpour, M., 2000, "Analysis and Synthesis of Human Motion From External Measurements," Proc. ICRA 2000, San Francisco, IEEE Robotic Society, New York, pp. 4015–4020.
 [7] Dariush, B., Hemami, H., and Parnianpour, M., 2000, "A Well-Posed, Embedded Constraint Representation of Joint Movement From Kinesiological Measurements," J. Biomech. Eng., **122**, pp. 437–445.
 [8] Dariush, B., Hemami, H., and Parnianpour, M., 2001, "Multi-Modal Analysis of Human Motion From External Measurements," J. Dyn. Syst., Meas., Control, **123**, pp. 272–278.
 [9] McCuskey, S., 1959, *An Introduction to Advanced Dynamics*, Addison-Wesley.
 [10] George, D., 1959, "Continuous Nonlinear Systems," Tech. Rep. 355, Research Laboratory of Electronics, Mass. Inst. of Technology, Cambridge, MA.
 [11] Zames, G., 1960, "Nonlinear Operators for System Analysis," Tech. Rep. 370, Research Laboratory of Electronics, Mass. Inst. of Technology, Cambridge, MA.
 [12] Smith, O., 1958, *Feedback Control Systems*, McGraw-Hill, New York.
 [13] Astrom, K. J., and Wittenmark, B., 1989, *Adaptive Control*, Addison-Wesley.
 [14] Kokotovic, P., Khalil, H. K., and O'Reilly, J., 1986, *Singular Perturbation Methods in Control*, Academic Press, New York.
 [15] Khalil, H., 1996, *Nonlinear Systems*, Prentice-Hall, Englewood Cliffs, N. J.
 [16] Barin, K., and Stockwell, C., 1986, "Parameter Estimation of a Model of Human Postural Control," Proc. of the Eighth Annual Conference of the IEEE/Engineering in Medicine and Biology Society, Forth Worth, Texas, Nov 7-10, 1986, IEEE, New York, pp. 1571–1574.
 [17] Barin, K., 1989, "Evaluation of a Generalized Model of Human Postural Dynamics and Control in the Sagittal Plane," Biol. Cybern. **61**, pp. 37–50.
 [18] Horak, F., and Nashner, L., 1986, "Central Programming of Postural Movements: Adaptation to Altered Support-Surface Configurations," J. Neurophysiol., **55**, pp. 1369–1381.
 [19] Brooks, V., 1986, *The Neural Basis of Motor Control*, Oxford University Press, New York.
 [20] Nashner, L., 1981, "Stance Posture in Humans," *Handbook of Behavioral Neurobiology*, A. L. Towe and E. Luschei, eds., Plenum Press, New York, pp. 527–566.
 [21] Bloch, A., 1994, *Hamiltonian and Gradient Flows, Algorithms and Control*, American Mathematical Society, Providence, Rhode Island.
 [22] Bullo, F., and Lewis, A., 2005, *Geometric Control of Mechanical Systems*, Springer, New York.
 [23] Hemami, H., and Katbab, A., 1982, "Constrained Inverted Pendulum for Evaluating Upright Stability," J. Dyn. Syst., Meas., Control, **104**, pp. 343–349.
 [24] Isidori, A., 1989, *Nonlinear Control Systems*, Springer-Verlag, Berlin.
 [25] Hemami, H., 1982, "A State Space Model for Interconnected Rigid Bodies," IEEE Trans. Autom. Control, **27**, pp. 376–382.
 [26] Hemami, H., 2002, "A General Framework for Rigid Body Dynamics, Stability and Control," J. Dyn. Syst., Meas., Control, **27** pp. 241–251.
 [27] Krstic, M., Kanellakopoulos, I., and Kokotovic, P., 1995, *Nonlinear Adaptive Control Design*, Wiley, New York.
 [28] Atherton, D. P., 1981, *Stability of Nonlinear Systems*, Research Studies Press, Chichester, UK.
 [29] Hemami, H., Wongchaisuwat, C., and Brinker, J. L., 1987, "A Heuristic Study of Relegation of Control in Constrained Robotic Systems," ASME J. Dyn. Syst., Meas., Control, **109**, pp. 224–231.
 [30] Kim, J., and Hemami, H., 1998, "Coordinated Three-Dimensional Motion of the Head and Torso by Dynamic Neural Networks," IEEE Trans. Syst., Man, Cybern., Part B: Cybern. **28**(5), pp. 653–666.